

Comparison of different ladder models

E. Jeckelmann*, D.J. Scalapino†, S.R. White*

*Department of Physics, University of California, Irvine, CA 92697

†Department of Physics, University of California, Santa Barbara, CA 93106

Using density matrix renormalization group calculations, we compare results obtained for the $t - J$, one-band Hubbard and three-band Hubbard models of a two-leg CuO ladder. Spin and charge gaps, pair binding energies, and effective pair hoppings are calculated for a wide range of parameters. All three models have an insulating state at a filling corresponding to one hole per Cu site. For physically relevant parameters their spin gaps are similar in size but they exhibit quite different charge gaps. We find that the binding energy of a pair of doped holes is of the order of the undoped ladder spin gap for all three models. The main difference between the models is the size of the effective pair hopping, which is significantly larger in the three-band model with parameters appropriate for CuO materials than in the other two models.

PACS Numbers: 74.20.Mn, 71.10.Fd, 71.10.Pm

The 2-leg CuO ladder materials have provided an interesting testing ground for ideas originally formulated to describe the 2D cuprates.¹ In particular, the undoped, 2-leg ladder material $SrCu_2O_3$ exhibits a spin gap² and the doped $(SrCa)_{14}Cu_{24}O_{41}$ ladder material³ can become superconducting under high pressure. The reduced dimensionality of this system has allowed for detailed numerical studies of both the $t - J$ and the one-band Hubbard models of a 2-leg ladder. In fact, it was a numerical Lanczos study⁴ of a 2-leg $t - J$ ladder which first suggested that the doped system might exhibit superconducting pairing. Since then, analytic calculations^{5,6} as well as density matrix renormalization group (DMRG) calculations⁷ on long one-band Hubbard ladders have shown the $d_{x^2-y^2}$ -like structure of the pairs and their power law correlations. Here we extend the DMRG approach to study a three-band Hubbard model of a CuO 2-leg ladder with the goal of comparing the $t - J$, one-band, and three-band Hubbard models.

The three-band Hubbard model we have studied has a hole Hamiltonian which can formally be thought of in terms of the “3-leg” ladder shown in Fig. 1. Alternating sites on the top and bottom legs have $Cu(d_{x^2-y^2})$ and $O(p_x)$ orbitals, while the center leg has $O(p_y)$ orbitals on the sites bridging the $Cu(d_{x^2-y^2})$ orbitals. With the orbital phase convention we have chosen, all the $O - Cu$ hopping matrix elements are $-t_{pd}$. The difference in the hole site energies is $\Delta = \varepsilon_p - \varepsilon_d$, and there is an onsite Cu Coulomb interaction U_d . The undoped system has one hole per Cu . In this state, if U_d is large compared to Δ , the charge gap is set by Δ and the system is said to be a charge gap insulator.⁸ Various parameter values have been suggested,⁹⁻¹² with typical ones having $\Delta/t_{pd} = 2$ to 3, $U_d/t_{pd} = 8$, and t_{pd} ranging from 1.3eV to 1.8 eV. Throughout this paper we will confine ourselves to an isotropic ladder and leave the case in which the rung parameters differ from the leg parameters to a future study.¹³

The 2-leg Hubbard model has a hopping $-t$ between the near neighbor ladder sites (along the legs and across the rungs) and an onsite Coulomb interaction U . Here

the undoped state corresponds to half-filling. At half-filling, the charge gap depends upon U and is said to be a Mott-Hubbard gap.⁸ Typical parameters⁹⁻¹² are $U/t = 10$ to 12 and $t = 0.4$ to 0.45eV.

The $t - J$ model has a near neighbor hopping term $-t$ with a restriction that no site can have two fermions. The exchange interaction in the $t - J$ model has the usual form

$$J \sum_{\langle ij \rangle} \left(\vec{S}_i \cdot \vec{S}_j - \frac{1}{4} n_i n_j \right) \quad (1)$$

with $\vec{S}_i = \frac{1}{2} c_{is}^\dagger \sigma_{ss'} c_{is'}$ and $n_i = c_{i\uparrow}^\dagger c_{i\uparrow} + c_{i\downarrow}^\dagger c_{i\downarrow}$. At half-filling, the $t - J$ model is just the Heisenberg 2-leg ladder and has an infinite charge gap. Typical parameters⁹⁻¹² are $J/t = 0.3$ and $t = 0.4$ to 0.5eV.

We use DMRG techniques¹⁴ to study long ladders (up to 64×2 sites in the $t - J$ and one-band Hubbard models and up to 16×2 Cu sites in the three-band Hubbard model) with open boundary conditions. DMRG has been shown to be a very accurate method to study ladder systems.^{7,13,15,16} Here we use up to 1200 states per block

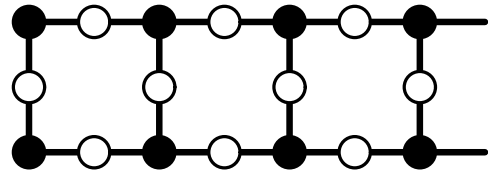


FIG. 1. Schematic of a CuO ladder. Here the solid circles represent $Cu(d_{x^2-y^2})$ orbitals and the open circles represent $O(p_x)$ orbitals along the upper and lower legs and $O(p_y)$ orbitals on the rungs. There is a hopping matrix element $-t_{pd}$ between the O and Cu sites as shown by the solid lines. The energy difference between the O and Cu sites is $\Delta = \varepsilon_p - \varepsilon_d$ and there is an onsite Cu Coulomb interaction U_d .

and extrapolate DMRG results for energies to extract the limit of zero truncation error and check the precision of our calculations.¹⁷ In addition, a few tests performed on small clusters with periodic boundary conditions show a perfect agreement with exact diagonalization results.¹⁸

We begin with the undoped ladder and calculate the spin gap

$$\Delta_s = E_0(S_z = 1) - E_0(S_z = 0) \quad (2)$$

Here Δ_s is the difference in energies between the spin 1 and spin 0 ground states. For the Heisenberg 2-leg ladder¹⁶

$$\Delta_s \simeq \frac{J}{2} \quad (3)$$

which is shown as the solid curve in Fig. 2, where we have plotted Δ_s versus $4t/J$. The dashed curve in Fig. 2 shows results for a 32×2 , half-filled Hubbard ladder. For large values of U/t , the Hubbard model at half-filling maps to the Heisenberg model with $J = 4t^2/U$. Thus in Fig. 2, the two curves approach each other at large values of U/t . Using twice the spin gap as a measure of the effective exchange interaction, we see from Fig. 2 that the strong coupling expression $J = 4t^2/U$ for the one-band Hubbard model overestimates the strength of the exchange interaction for physically relevant values of the parameters. However, we can use Δ_s as a unit of energy in comparing the $t - J$ and one-band Hubbard models, each in their relevant physical parameter regimes. Thus, for an infinite 2-leg ladder, the $t - J$ model with $J/t = 0.3$ has $\Delta_s/t \cong 0.15$ while the one-band Hubbard model with $U/t = 12$ has $\Delta_s/t \cong 0.12$ as seen in Table 1. Taking $t = 0.45\text{eV}$, twice these spin gap energies give reasonable effective exchange couplings of 0.135eV (1600K) and 0.11eV (1300K) for the $t - J$ and one-band Hubbard ladders, respectively. Naturally, either of these two could be further adjusted by using a different value of t , but our point is simply that they are in the correct range. We also note that the spin gap $\Delta_s/t \cong 0.11$ of the one-band Hubbard model with $U/t = 6$ is similar to the value obtained for $U/t = 12$ (see Table 1).

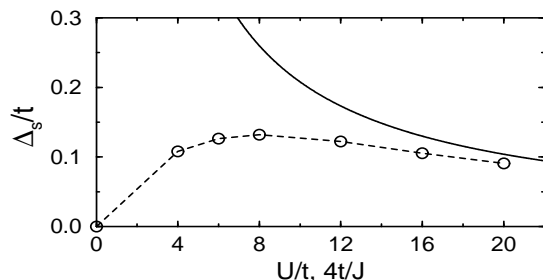


FIG. 2. The spin gap Δ_s/t versus $4t/J$ for the $t - J$ (Heisenberg) model (solid line) and U/t for the one-band Hubbard model (dashed line) at half-filling on a 32×2 ladder.

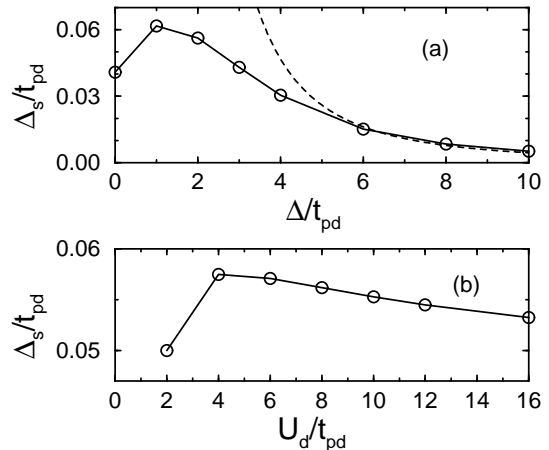


FIG. 3. (a) The spin gap Δ_s/t_{pd} versus Δ/t_{pd} for the 3-band Hubbard model at a filling of one hole per Cu , with $U_d/t_{pd} = 8$. The dashed line is the strong coupling limit, Eq. (4). (b) The spin gap energy Δ_s versus U_d/t_{pd} with $\Delta/t_{pd} = 2$ for the 3-band Hubbard model at a filling of one hole per Cu . All results are for an 8×2 Cu ladder.

Results for the spin gap Δ_s of the three-band Hubbard model at a filling of one hole per Cu are shown in Figs 3(a) and (b). In Fig. 3(a), Δ_s/t_{pd} is plotted versus Δ/t_{pd} for a ladder containing 8×2 Cu sites with $U_d/t_{pd} = 8$. In strong coupling, the $Cu - Cu$ exchange interaction has the form

$$J_{cu} = 4 \left(\frac{t_{pd}^2}{\Delta} \right)^2 \left[\frac{1}{U_d} + \frac{1}{\Delta} \right] \quad (4)$$

The dashed curve in Fig. 3(a) shows $J_{cu}/2$ and one sees that the spin gap of the three-band model approaches the strong coupling $J_{cu}/2$ result at large values of the $\Delta = \varepsilon_p - \varepsilon_d$ splitting. However, just as for the one-band Hubbard model, the strong-coupling expression for the exchange interaction substantially overestimates it in the physically relevant region of parameters. The dependence of Δ_s on U_d/t_{pd} for $\Delta/t_{pd} = 2$ is shown in Fig. 3(b). At large values of U_d/t_{pd} , the exchange is dominated by the Δ term in Eq. (4) as expected for a charge transfer insulator. Taking $\Delta/t_{pd} = 2$ and $U_d/t_{pd} = 8$ we find that Δ_s/t_{pd} extrapolates to $\cong 0.035$ for an infinite CuO ladder (see Table 1), which for $t_{pd} = 1.5\text{eV}$ gives $J_{cu} \equiv 2\Delta_s \cong 0.11\text{eV}$ (1300K). Thus, even though the region of relevant physical parameters does not lend itself to a simple strong coupling expansion which relates the three models, the spin gaps for the three models are in fact similar in size and provide a useful energy scale describing the strength of the exchange coupling.

The charge gaps for the insulating (undoped) phases, however, are quite different. The insulating state of the $t - J$ model has an infinite charge gap reflecting the constraint that no site can have two fermions. In the Hubbard models, the charge gap is defined by

$$\Delta_c = (E_0(2) + E_0(-2) - 2E_0(0)) / 2, \quad (5)$$

where $E_0(n)$ is the ground state energy of a ladder with n holes relative to the undoped ladder. The charge gaps for the half-filled, one-band Hubbard model and the three-band Hubbard model with one hole per Cu are plotted versus the onsite Coulomb interaction in Fig. 4(a). At large values of U , the charge gap in the one-band Hubbard model varies as U , while as expected, the charge gap of the three-band Hubbard model saturates at a value set by Δ when U_d becomes very large. As noted above, the spin gap energy provides a useful unit of energy in comparing the different models. In Table 1 we show the charge gap in units of the spin gap in the one-band Hubbard model for $U/t = 6$ and 12 and in the three-band Hubbard model for the physical parameters $\Delta/t_{pd} = 2$ and 3 with $U_d/t_{pd} = 8$. One can use either $U/t = 6$ or 12 to reproduce the three-band model Δ_c/Δ_s ratio depending on the value of Δ/t_{pd} . Taking the same values of t and t_{pd} as above, we obtain $\Delta_c = 1.4$ to 3.9 eV. The experimental value of the charge gap is still debated¹¹ but is of the same order of magnitude (2-5eV).

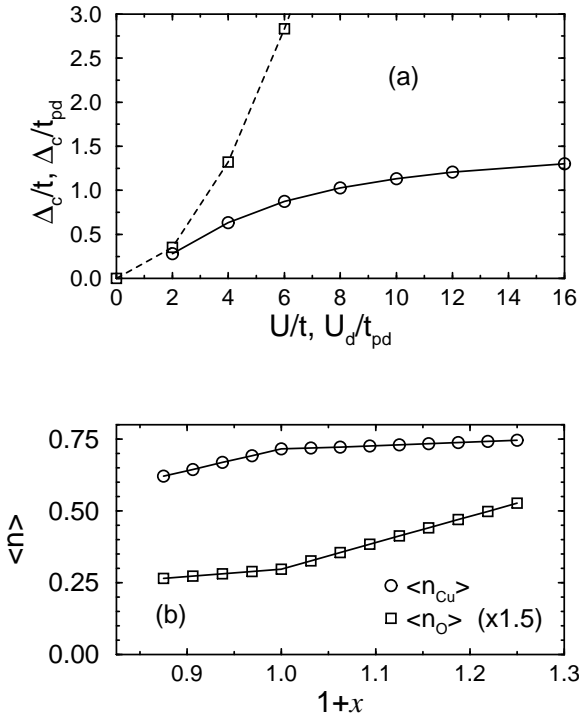


FIG. 4. (a) The charge gap Δ_c versus U/t for the one-band (dashed) Hubbard model on a 32×2 ladder and versus U_d/t_{pd} for the three-band (solid) Hubbard model with $\Delta/t_{pd} = 2$ on a ladder containing 8×2 Cu sites. Note that Δ_c is measured relative to t for the one-band Hubbard model and relative to t_{pd} for the three-band Hubbard model. (b) The hole occupation per Cu ($\langle n_{Cu} \rangle$) and O ($\langle n_O \rangle$) versus the hole concentration $1+x$ per $CuO_{1.5}$ unit cell on a ladder containing 16×2 Cu sites with $U_d/t_{pd} = 8$ and $\Delta/t_{pd} = 2$.

The “charge transfer gap” behavior of the three-band model is also seen in Fig. 4(b) where we have plotted the hole occupation per Cu and per 1.5 O versus the hole concentration $1+x$ per $CuO_{1.5}$ unit cell for the physical parameters $U_d/t_{pd} = 8$ and $\Delta/t_{pd} = 2$. For $x < 0$, the holes go primarily onto the Cu sites (72% of the hole density is on these sites) while for $x > 0$, the O sites are favored with 88% of the additional hole density going to these sites. For example, for $x = 0.25$, the average hole density on the Cu site is increased by only 0.03 (4%) while that on an oxygen site is increased by about 0.15 (77%), or 0.22 per $O_{1.5}$, from the result for the undoped ladder ($x = 0$). This behavior can easily be understood. For $x \leq 0$, only Cu orbitals are occupied because they have lower energy than the O orbitals. (The hybridization of the Cu and O orbitals due to the finite hopping t_{pd} is responsible for the fractional density on Cu and O sites.) For $x > 0$, all Cu orbitals are occupied by at least one hole. The energy to put a second hole on one of these orbitals is set by U_d , while the energy to put a hole on the O orbitals is set by Δ . Thus, for the parameters considered here ($\Delta < U_d$), additional holes go onto O orbitals. In the opposite limit $U_d < \Delta$, we have found that holes go primarily on Cu orbitals for $x > 0$, as expected.

It is interesting to note that magnons also go primarily on Cu sites (76% of the spin density is on these sites). This distribution is very close to the hole distribution of the undoped ladder and remains constant for all doping studied $-0.125 \leq x \leq 0.25$. This result suggests that low-energy spin excitations involve only unpaired holes in (hybridized) Cu orbitals even when $x \neq 0$. According to Zhang and Rice¹⁹, each doped hole is locked in a singlet state with another holes in a Cu orbital and does not contribute to spin excitations at low energy. Our results certainly support this scenario although it is not obvious that their argument based on a CuO_4 cluster is valid for the lattice configuration shown in Fig. 1.

Next we consider the two-hole pair binding, defined by

$$\Delta_{pb} = E_0(2) + E_0(0) - 2E_0(1) \quad (6)$$

if the quantity on the right-hand side is positive and $\Delta_{pb} = 0$ otherwise. It should be noted that the dependence of the pair binding energy on system size is significant. Moreover, Δ_{pb} generally increases when the ladder length increases, while other quantities, such as the spin gap, decrease. Therefore, when comparing values of Δ_{pb} one should always keep the corresponding system size in mind. In Fig. 5(a) Δ_{pb} is plotted versus $4t/J$ for the $t-J$ model and U/t for the one-band Hubbard model on a 32×2 ladder. Just as previously found for the spin gap, the pair binding energy for the $t-J$ model approaches that of the one-band Hubbard model at large values of U/t . Furthermore, although the two models have very different charge gaps, the scale of their pair binding energies in the physically relevant parameter region is set by Δ_s . This is clearly illustrated in Fig. 5(b), where we

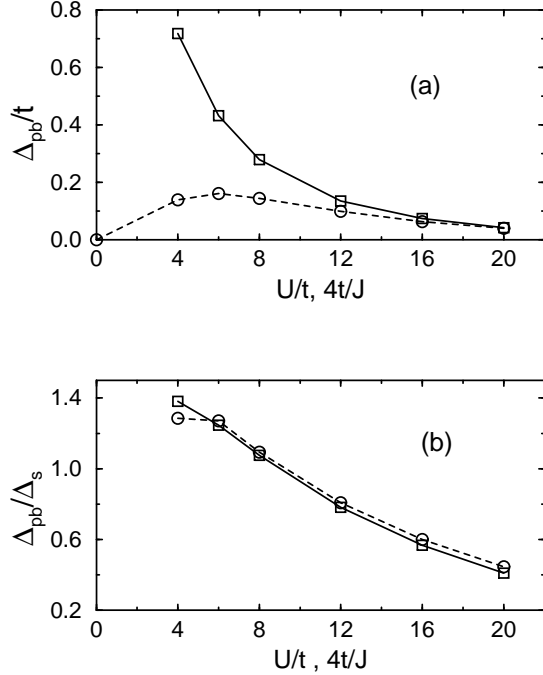


FIG. 5. (a) The hole pair binding energy Δ_{pb}/t versus $4t/J$ for the $t-J$ model (solid) and U/t for the one-band Hubbard model (dashed) on a 32×2 ladder. (b) The ratio Δ_{pb}/Δ_s in both models.

show the pair binding energy in units of the spin gap as a function of U/t in the one-band Hubbard model and as a function of $4t/J$ in the $t-J$ model on a 32×2 ladder. We note that the ratio Δ_{pb}/Δ_s is surprisingly similar in both models despite the widely different behavior of Δ_{pb} and Δ_s shown in Figs. 2 and 5(a). As previously discussed,^{7,15} the pair wave function for both of these models has a $d_{x^2-y^2}$ -like form. Moreover, we have found that the structure of single holes and hole pairs in the one-band Hubbard model with $U/t = 8$ is identical to those observed in the $t-J$ model.²⁰

Results for the pair binding energy of the three-band Hubbard model are shown in Figs 6(a) and (b). For $U_d/t_{pd} = 8$, the pair binding peaks for $\Delta/t_{pd} \cong 2$ and as shown in Fig. 6(b), the pair binding energy increases as U_d/t_{pd} increases. Similar results for a Cu_4O_8 cluster were found from Lanczos calculations.^{18,21} More recently, Martin²² has discussed pairing on small clusters in terms of rehybridization associated with the charge-transfer channels. A recent Quantum Monte Carlo study of the three-band Hubbard model²³ yields similar results for clusters with up to 6×6 Cu sites. For the physical range of parameters appropriate to the cuprates, one also has $\Delta_{pb} \sim \Delta_s$ in the three-band model. However, the ratio Δ_{pb}/Δ_s extrapolated for a ladder of infinite length is clearly larger than in both other models with their typical parameters, as shown in Table 1. A better agreement with the three-band Hubbard model results is obtained

by taking $U/t = 6$ for the one-band Hubbard model. In addition, in the three-band Hubbard model the hole pair wave function has a $d_{x^2-y^2}$ -like form as determined from measurements of the rung-rung and rung-leg pair field correlations.

We have also measured the pair binding energy versus the hole concentration x relative to the undoped ladder. In this case the pair binding energy is defined by

$$\Delta_{pb}(x) = E_0(2n) + E_0(2n-2) - 2E_0(2n-1), \quad n > 0 \quad (6')$$

$$\Delta_{pb}(x) = E_0(2n) + E_0(2n+2) - 2E_0(2n+1), \quad n < 0 \quad (6'')$$

Here x is equal to $2n$ divided by the number of holes in the undoped ladder. Results for the pair binding energy Δ_{pb} relative to the undoped spin gap Δ_s are shown in Fig. 7(a) for the three models. There is no striking difference between the three models for $x > 0$. We note, however, that while the Hubbard model is particle-hole symmetric about half-filling, one can only add holes to the $t-J$ model and we find no evidence for pair binding for $x < 0$ in the 3-band Hubbard model with $U_d/t_{pd} = 8$ and $\Delta/t_{pd} = 2$. We are not sure of the exact nature of the ground state of the three-band Hubbard model with less than one hole per Cu site. In fact, we have not been able to investigate this regime as thoroughly as the $x \geq 0$ regime because density matrix renormalization group calculations are much harder and less accurate in this case. However, our numerical simulations strongly suggest that the $x < 0$ and $x > 0$ regimes are quite different. As noted previously, holes go primarily on Cu orbitals for $x < 0$ while doped holes are on O orbitals for $x > 0$ (see Fig. 4(b)). Thus, it is possible that the effective interactions between doped particles are different for both regimes.

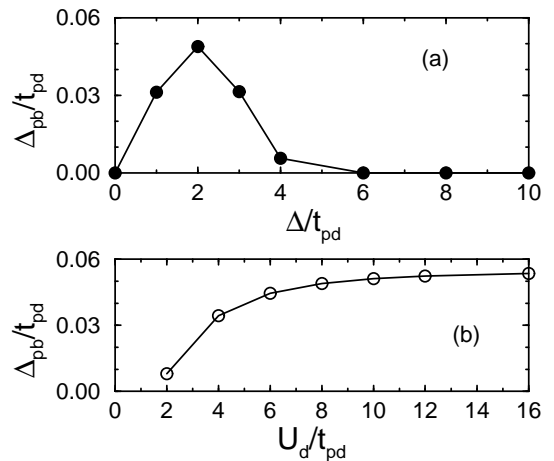


FIG. 6. (a) The pair binding energy Δ_{pb} versus Δ/t_{pd} with $U_d/t_{pd} = 8$ for the 3-band Hubbard model. (b) The pair binding energy versus U_d/t_{pd} with $\Delta/t_{pd} = 2$ for the 3-band Hubbard model. These calculations are for an 8×2 Cu ladder.

TABLE I. Spin gap Δ_s (in units of the bare hopping term t or t_{pd}), and charge gap Δ_c , pair binding energy Δ_{pb} , effective pair hopping t_{eff} and effective magnon hopping v_{eff} (in units of the spin gap) obtained by extrapolating to a ladder of infinite length.

Model	Parameters	Δ_s	Δ_c/Δ_s	Δ_{pb}/Δ_s	t_{eff}/Δ_s	v_{eff}/Δ_s
$t - J$	$J/t = 0.3$	0.151	∞	0.71	2.4	5.0
1-band	$U/t = 12$	0.116	70	0.83	5.4	8.5
1-band	$U/t = 6$	0.111	25	1.4	12	24
3-band	$\Delta/t_{pd} = 3, U_d/t_{pd} = 8$	0.030	58	1.2	12	7.5
3-band	$\Delta/t_{pd} = 2, U_d/t_{pd} = 8$	0.035	29	1.6	18	11

The decrease in the pair binding energy with x correlates with the decrease in the near-neighbor spin-spin correlations $\langle \vec{S}_i \cdot \vec{S}_j \rangle$ shown in Fig. 7(b). (Note that for the three-band Hubbard model we show the spin-spin correlations between near-neighbor Cu sites.) Thus, the decrease in the pair binding energy with increased hole concentration reflects the destruction of the underlying exchange correlations by the added holes. It should be noted that the differences between the values of $\langle \vec{S}_i \cdot \vec{S}_j \rangle$ in the three models are mostly due to the increase of charge fluctuations in going from the $t - J$ model to the one-band Hubbard model and then to the three-band Hubbard model. These charge fluctuations reduce the local

magnetic moments $\langle \vec{S}_i^2 \rangle$ and thus the absolute value of $\langle \vec{S}_i \cdot \vec{S}_j \rangle$. However, as noted previously, the effective exchange coupling between spins is similar in the three models.

We have also calculated the effective hopping parameter t_{eff} of a hole pair from the dependence of the pair energy obtained in ladders of different lengths. We define the pair energy by

$$\varepsilon_p = E_0(2) - E_0(0). \quad (7)$$

In ladders with open boundary conditions, the energy of the pair varies as

$$\varepsilon_p(L_{eff}) = \varepsilon_p(\infty) + t_{eff} \left(\frac{\pi}{L_{eff} + 1} \right)^2 \quad (8)$$

where the effective system length L_{eff} differs from the actual ladder length L because of end effects. For a given system, L_{eff} can be determined from the wavelength $\lambda = 2(L_{eff} + 1)$ of the charge density distribution of the pair. Fig. 8 shows a plot of the ground state energy of a hole pair versus $(L_{eff} + 1)^{-2}$ for the three different models. t_{eff} is equal to the slope of the lines in Fig. 8 divided by π^2 . We have found that the difference $\delta L = L_{eff} - L$ tends to a constant for large systems. Thus, in practice we can substitute $L + \delta L$ for L_{eff} in Eq. 8 and use δL as a fit parameter.

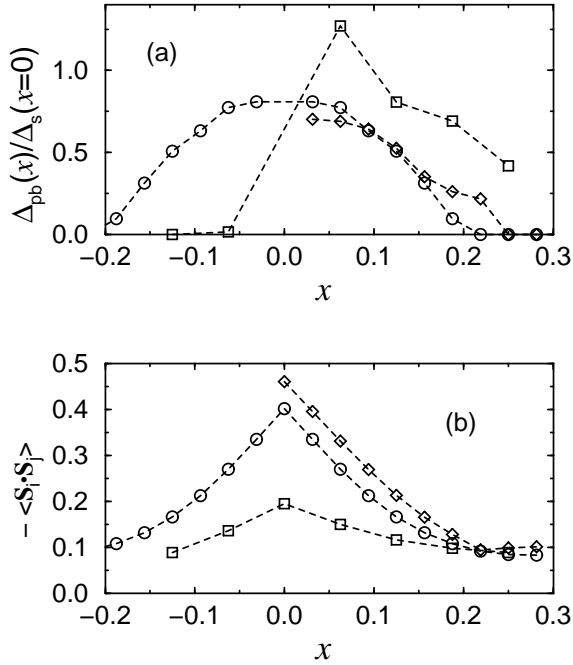


FIG. 7. (a) The ratio of the pair binding energy to the undoped spin gap versus hole doping. The diamonds are for a 32×2 $t - J$ ladder with $J/t = 0.3$. The circles are for a one-band 32×2 Hubbard ladder with $U/t = 12$. The squares are for the three-band Hubbard model with $U_d/t_{pd} = 8$ and $\Delta/t_{pd} = 2$ on a 16×2 Cu ladder. (b) The near-neighbor Cu spin-spin correlation function $\langle \vec{S}_i \cdot \vec{S}_j \rangle$ versus x for the three models.

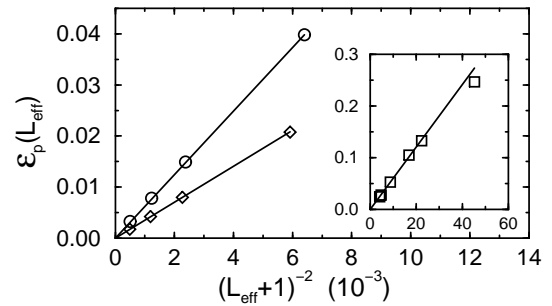


FIG. 8. Plot of the hole pair energy versus $(L_{eff} + 1)^{-2}$ for the three different models. The notation is the same as in Fig. 7. Actual ladder lengths L range from 5 to 16 Cu sites in the three-band Hubbard model and from 16 to 48 for the two other models. For each model, the zero of the energy has been set to the extrapolated value of the pair energy.

In Table 1, we list t_{eff} normalized with respect to Δ_s for the $t-J$, and the one- and three-band Hubbard models with $J/t = 0.3$, $U/t = 6$ and 12 , and $U_d/t_{pd} = 8$, $\Delta/t_{pd} = 2$ and 3 , respectively. We have also listed the pair binding energy Δ_{pb} in units of the spin gap energy Δ_s . Now, as previously discussed, the spin gap in the insulating case is of order $J/2$ and it sets the scale of the pair binding energy so that Δ_s and Δ_{pb} for the three models are quite similar. However, the pair dispersion is enhanced in going from the $t-J$ model to the one-band Hubbard model and further enhanced for the three-band Hubbard model if one uses parameters appropriate for *CuO* materials. We believe that this enhancement is associated with the additional charge fluctuations which the one and three-band Hubbard models allow. The large enhancement in the three-band model reflects the fact that its charge gap is set by Δ when U_d is large rather than U_d . In Fig. 9 we show the effective pair hopping as a function of U/t in the one-band Hubbard model and as a function of $4t/J$ in the $t-J$ model. In the $t-J$ model it seems that the effective pair hopping is always small ($t_{eff}/t < 0.4$). In the one-band Hubbard model, however, the pair dispersion is strongly enhanced as U/t decreases and for $U/t = 6$ the ratio t_{eff}/Δ_s is similar to the value obtained in the three-band Hubbard model with $\Delta/t_{pd} = 3$ and $U_d/t_{pd} = 8$ (see Table 1). For large values of U/t , the pair dispersion of the one-band Hubbard model approaches that of the $t-J$ model as shown in Fig. 9. However, the difference between the pair dispersion in both models seems to be of the order $4t/U$ when $U \rightarrow \infty$. This difference could be due to next-nearest-neighbor hopping terms of the order $4t/U$ which are neglected in the derivation of the $t-J$ model from the strong-coupling limit of the Hubbard model.

An effective magnon hopping v_{eff} can be calculated from the dependence of the spin gap on the ladder length. We use Eq. 8 with v_{eff} and Δ_s substituted for t_{eff} and ϵ_p , respectively. In this case the effective ladder length is determined from the spin density profile. In Table 1 v_{eff} normalized with respect to Δ_s is listed for undoped ladders.

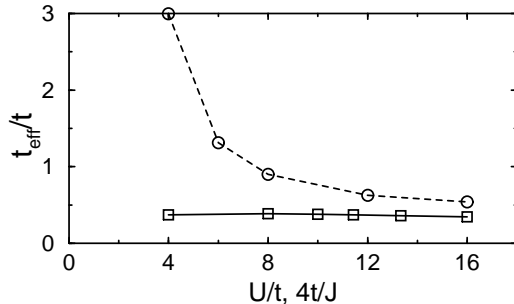


FIG. 9. The effective hopping parameter for two holes is shown by the circles for the one-band Hubbard model and by the squares for the $t-J$ model.

The values of v_{eff}/Δ_s obtained in the three models are of the same order of magnitude for the physically relevant parameters. We note that in this case the value obtained in the one-band Hubbard model with $U/t = 6$ is much larger than the other results. In undoped ladders the effective magnon hopping obtained for the one-band Hubbard model approaches the result found in the $t-J$ (Heisenberg) model, $v_{eff} \cong 2.5J$, at large values of U/t as expected. A recent perturbation calculation of two-leg Heisenberg ladders²⁴ gives $v_{eff} \cong 2$, in satisfactory agreement with our numerical result.

To summarize, all three models of course have a spin gap in the undoped phase. Furthermore, the parameters for the different models can be chosen to make these spin gaps comparable and in the correct physical regime. As noted, however, these three models have very different charge gaps with the $t-J$ model having an infinite charge gap, the one-band Hubbard model having a Mott-Hubbard gap set by U and the three-band *CuO* model having a charge transfer gap set by $\Delta = \epsilon_p - \epsilon_d$ for the physical parameter range of interest. The binding energy of two added holes is basically set by the spin gap. However, $\Delta_{pb}/\Delta_s \cong 0.7$ to 0.8 for the $t-J$ and one-band Hubbard ladder while $\Delta_{pb}/\Delta_s \cong 1.2$ to 1.6 for the three-band Hubbard ladder with parameters appropriate for *CuO* materials. Thus the hole pairs are in fact bound more tightly in units of the spin gap energy in the three-band Hubbard ladder. The main difference between the models is the size of the effective pair hopping which is significantly larger in the three-band model for the physical parameters. It is often assumed that these three models with parameters and band-fillings appropriate for *CuO* materials describe the same low-energy physics. Our study has not revealed any fact which explicitly contradicts this point of view. However, our results show that neither the one-band Hubbard model nor the $t-J$ model can reproduce all the three-band Hubbard model results with a single set of effective parameters. For instance, it seems that the pairing properties are better reproduced by the one-band Hubbard model with $U/t = 6$ than with the usual parameters $U/t = 12$.

Finally, we believe that the larger dispersion signified by the effective pair hopping, which we found for the three-band Hubbard model, points to an important feature of the physics contained in the charge transfer insulator. Pairs are less likely to localize in the three-band Hubbard model than in the other models for the physical parameters. This could have a significant effect in a two-dimensional lattice. For instance, in the two-dimensional $t-J$ model doped holes tend to form ordered arrays called stripes, which seem to suppress superconductivity, at least when the stripes are static.²⁵ A study of a three-leg ladder using both density matrix renormalization group methods and quantum Monte Carlo simulations has shown that similar stripes also appear in the one-band Hubbard model for $U/t > 6$, but not for weaker coupling.¹⁷ Thus, it seems that the sharp increase of pair mobility observed for decreasing U/t in the two-leg lad-

der correlates with a transition from a striped ground state to a ground state without stripes in wider ladders. Therefore, we think that the larger charge fluctuations which the three-band Hubbard model allows (compared to the $t - J$ model) should lead in the two-dimensional lattice to a reduced tendency for domain walls to lock up in static arrays with suppressed superconductivity.

ACKNOWLEDGMENTS

We thank R.L. Martin for helpful discussions. DJS acknowledges support from the Department of Energy under grant DE-FG03-85ER-45197. DJS would also like to acknowledge the Program on Correlated Electrons at the Center for Material Science at Los Alamos National Laboratory. SRW wishes to acknowledge the support of the Campus Laboratory Collaborations Program of the University of California and from the NSF under Grant No. DMR-9509945. EJ thanks the Swiss National Science Foundation for financial support.

- ¹⁸ M. Ogata and H. Shiba, J. Phys. Sci. Jpn **57**, 3074 (1988).
- ¹⁹ F.C. Zhang and T.M. Rice, Phys. Rev. B **37**, 3759 (1988).
- ²⁰ S.R. White and D.J. Scalapino, Phys. Rev. B **55**, 6504 (1997).
- ²¹ J.E. Hirsch, E. Loh, D.J. Scalapino and S. Tang, Phys. Rev. B **39**, 243 (1996).
- ²² R.L. Martin, Phys. Rev. B **54**, R9647 (1996).
- ²³ M. Guerrero, E. Gubernatis and S. Zhang, cond-mat/9711125.
- ²⁴ J. Piekarewicz and J.R. Shepard, cond-mat/9804261.
- ²⁵ S.R. White and D.J. Scalapino, Phys. Rev. B **55**, 14701 (1997); Phys. Rev. B **57**, 3031 (1998); Phys. Rev. Lett. **80**, 1272 (1998).

-
- ¹ E. Dagotto and T.M. Rice, Science **271**, 618 (1996).
 - ² M. Takano, *et. al.*, Jpn. J. Appl. Phys. **1**, 3 (1992).
 - ³ M. Uehara, *et. al.*, J. Phys. Soc. Jpn. **65**, 2764 (1996).
 - ⁴ E. Dagotto, J. Riera, and D.J. Scalapino, Phys. Rev. B **45**, 5744 (1992).
 - ⁵ S. Gopalan, T.M. Rice, and M. Sigrist, Phys. Rev. B **49**, 8901 (1994).
 - ⁶ L. Balents and M.P.A. Fisher, Phys. Rev. B **53**, 12133 (1996).
 - ⁷ R. Noack, D.J. Scalapino, and S.R. White, Phil. Mag. B **74**, 485 (1996).
 - ⁸ J. Zaanen, G.A. Sawatzky, and J.W. Allen, Phys. Rev. Letters **55**, 418, (1985).
 - ⁹ M.S. Hybertsen, E.B. Stechel, M. Schluter, and D.R. Jennison, Phys. Rev. B **41**, 11068 (1990).
 - ¹⁰ A.K. McMahan, J.F. Annett, and R.M. Martin, Phys. Rev. B **42**, 6268 (1990).
 - ¹¹ R.L. Martin, Phys. Rev. B **53**, 15501 (1996).
 - ¹² O.K. Andersen, O. Jepsen, A.I. Liechtenstein, and I.I. Mazin, Phys. Rev. B **49**, 4145 (1994).
 - ¹³ The case in which the hopping parameter on a rung is different from that along the legs has been studied for the 2-leg Hubbard model. R.M. Noack, N. Bulut, D.J. Scalapino, and M.G. Zacher, Phys. Rev. B **56**, 7162 (1997).
 - ¹⁴ S.R. White, Phys. Rev. Lett. **69**, 2863 (1992); Phys. Rev. B **48**, 10345 (1993); Phys. Rev. Lett. **77**, 3633 (1996).
 - ¹⁵ R.M. Noack, S.R. White, and D.J. Scalapino, Phys. Rev. Lett. **73**, 882 (1994).
 - ¹⁶ S.R. White, R.M. Noack, and D.J. Scalapino, Phys. Rev. Lett. **73**, 886 (1994).
 - ¹⁷ J. Bonca, J.E. Gubernatis, M. Guerrero, Eric Jeckelmann, and Steven R. White, cond-mat/9712018.